Porous PVDF Monoliths with Templated Geometry

Suzana Djeljadini, Patrick Bongartz, Michael Alders, Nils Hartmann, Alexander Oing, Christian Cornelissen, Felix Hesselmann, Jutta Arens, Ulrich Steinseifer, John Linkhorst, and Matthias Wessling*

Additive manufacturing of complex porous polymer geometries is a new field of advanced materials processing. Such new geometries can be used to fabricate porous polymer monoliths serving as a support for other material functions. Here, a novel fabrication technology to manufacture tailored 3D porous monoliths via additive manufacturing and templating is presented. The method is based on replicating a 3D-printed mold with a polymer solution of polyvinylidenfluorid-triethyl phosphate (PVDF-TEP) and induce phase separation of the polymer solution subsequently. In a second step, the mold is removed without affecting the porous PVDF phase. As a result, porous monoliths with a templated 3D architecture are successfully fabricated. The manufacturing process is successfully applied to complex structures and can be applied to any conceivable geometry. Coating the porous 3D monoliths with another PVDF solution allows applying a skin layer yielding an asymmetric membrane monolith. As a showcase, a polydimethylsiloxane coating even leads to a smooth and dense layer of micrometer size. The methodology enables a new generation of complex porous polymer monoliths with tailored surface coatings. For the combination of poly(dimethylsiloxane) on a porous support, gas/liquid mass transfer is used in blood oxygenation with reduced diffusion limitation is within reach.

1. Introduction

Membrane performance is an essential factor in developing and applying membrane technology to face global challenges in water, energy and healthcare. For the latter, the development of artificial organ-like devices with improved mass transport is a challenge to replace or support essential body functions such as blood dialysis and blood oxygenation.

The design of gas-liquid membrane contactors as blood oxygenation devices with improved rates of oxygenation and CO_2-removal is limited by the diffusion in the gas-wetted membrane phase as well as the blood-side liquid phase diffusion resistance. While the first required low resistance can be overcome by high porosity and thin membrane thickness (a challenge we currently aim to solve for the proposed monolithic geometries), the second one can be solved using intricate flow channel geometries, which create secondary flows destabilizing diffusion boundary layers. Lately, the availability of new and advanced manufacturing methods has allowed a more radical rethinking of membranes and membrane geometries, shaping the blood-side channel flow conditions. Some of our work in the field of engineered fluid flow conditions, imposed by engineered channel geometries or membrane geometries, comprise static mixers to prevent rejection-induced colloidal accumulation and subsequent fouling,[1–4] aerating static mixers to even further improve shear-rate induced fouling prevention,[5] staggered herringbone structures to improve gas transport in G/L mass transfer in microfluidic chips and reactors,[6,7] as well as twisted[8] and sinusoidal hollow fiber shaped membranes.[9,10]

First steps towards the direct fabrication of free-form 3D membranes have been taken.[11] So far, 3D printing was applied

S. Djeljadini, P. Bongartz, M. Alders, N. Hartmann, A. Oing,
Dr. C. Cornelissen, F. Hesselmann, Prof. J. Arens, Prof. U. Steinseifer,
Dr. J. Linkhorst, Prof. M. Wessling
RWTH Aachen University, Chemical Process Engineering
Forckenbeckstr. 51, 52074 Aachen, Germany
E-mail: manuscripts.cvt@avt.rwth-aachen.de

The ORCID identification number(s) for the author(s) of this article can be found under https://doi.org/10.1002/admt.202100325.

S. Djeljadini, Prof. M. Wessling
DWI Leibniz-Institute for Interactive Materials
Forckenbeckstr. 50, 52074 Aachen, Germany

Dr. C. Cornelissen
RWTH Aachen University Hospital, Department of Pneumology
and Internal Intensive Care Medicine, Medical Clinic V
Pauwelsstr. 30, 52074 Aachen, Germany

F. Hesselmann, Prof. J. Arens, Prof. U. Steinseifer
RWTH Aachen University, Cardiovascular Engineering, Institute
of Applied Medical Engineering, Helmholtz Institute
Pauwelsstr. 20, 52074 Aachen, Germany

Prof. J. Arens
University of Twente, Chair of Engineering Organ Support Technologies
Department of Biomechanical Engineering
De Horst 2, Enschede 7522LW, The Netherlands

**ADVANCED
SCIENCE NEWS**
www.advancedsciencenews.com

**ADVANCED
MATERIALS
TECHNOLOGIES**
www.advmattechnol.de

in the design of membrane modules, spacers, static mixers, or even the membrane itself.[12,13]

Femmer et al. used the 3D printing technique to develop complex membrane geometries. These complex-shaped membranes were designed based on 'triply periodic minimal surfaces' (TPMS), which are based on a local area minimization principle resulting in a smooth local topology with constant mean curvature.[14] They showed that these structures could be applied for heat and mass transport.[15,16] Moreover, they could show that the novel TPMS membrane geometries outperformed flat-sheet and HF in heat transport and demonstrated exceptional mass transport for TPMS gas-liquid contactor devices.[6] Membrane oxygenators strongly rely on miniaturization with the following design challenges: a) miniaturization of the blood hold-up volume, b) maximize effective membrane packing density (m^2 m^{-3}), c) minimize the membrane resistance, and d) maximum mass transfer at the membrane interface by destabilizing the laminar boundary layers at the membrane/fluid interface.[17] Current 3D-printed membranes do not comply with these prerequisites.[16] These 3D membranes are made from poly(dimethylsiloxane) (PDMS), an excellent suitable material for blood oxygenation. However, due to fabrication limitations and the necessity for mechanical strength, the wall thickness of these membranes is too high (1mm). This membrane thickness contributes significantly to mass transport resistances, hence leading to a reduced mass transport rate. In comparison, commercially available oxygenators are based on porous hollow fiber membrane with porosity being a prerequisite for only membrane-related mass transport resistance.[18,19]

Until now, the 3D printing technology cannot print porous membranes or porous monolithic structures that can serve as a membrane support. [13] There have been attempts to print the pores of a membrane directly. Still, either the resolution or the build size of 3D printers remains so far a limitation for the practical fabrication of porous membranes.[20,21] It is therefore highly desired to prove that porous 3D membrane structures can be fabricated with a first strategy presented here by printing a 3D mold and templating the porous membrane within this mold. If this porous architecture is thin, we call it a membrane, otherwise with thicker walls it should be a monolithic support structure.

Two decades ago, porous polymeric monoliths were fabricated with a simple molding process prepared by polymerization inside a tubular closed mold[22,23] imposing the outer geometry through the geometry of the mold geometry. These monoliths allowed a paradigm change from classical beads used in chromatography columns toward a single polymer piece with enhanced properties.[24] Templating or printing such monolithic materials is not straightforward. Porous TPMS electrodes have been made by direct additive manufacturing through the printing of slurries.[25] Only recently, a direct printing method for photopolymerization was disclosed and even for TPMS geometries.[26] However, we aim at processing materials known to be used in biomedical applications, in particular for materials that are hemocompatible.

In this work, we bridge the gap between the limitations in 3D printing resolution and typical membrane fabrication processes by combining the molding process with the classical membrane fabrication process: a non-solvent induced phase separation (NIPS) process of a polymer solution within 3D-printed molds serving as the template for the channel system. NIPS is a common and commercially widely used technology in membrane manufacturing, thanks to its versatility allowing a great variety of membrane architectures.[27] So far, the NIPS technology has only been applied to flat sheet and hollow fiber membranes. With the proposed method, we transfer the NIPS technology towards freedom of design fabrication of hierarchical porous monoliths and membranes. We showcase this materials processing platform using PVDF, which is known for its hydrophobic nature, good chemical and thermal stability, and in particular good biocompatibility, which makes it interesting for membrane contactor applications like blood oxygenation processes.[28,29]

To fabricate porous monolithic supports for membrane functionality, we propose to use 3D printed molds as a template, fill the template with a PVDF polymer solution, and finally perform a non-solvent induced phase separation as visualized in **Figure 1**. After a successful phase inversion, the mold can be dissolved without impairing the porous PVDF. As done in the engineering of ceramic multi-layer membranes, these porous 3D-templated bodies can be further functionalized with additional functional layers. For the application of G/L exchange, we propose to coat a) an additional PVDF layer to establish a hierarchical asymmetric membrane monolith and b) a dense but gas permeable PDMS coating on top of the composite PVDF monolith to obtain a pore-free layer avoiding liquid entry into the porosity. This methodology can produce tailored geometries of thin-film composite membranes for gas-liquid contactor devices. When using other coating solutions, different functionalities can be obtained, adding to the versatility of the methodology.

2. Results and Discussion

2.1. NIPS Process of Monolith Bodies

Many membrane formation processes are based on the so-called phase inversion process, which utilizes a ternary system composed of a polymer, solvent, and precipitant.[30] The choice of components offers a great variety of combinations and thus offers a wide property spectrum for membrane fabrication. Additives can be added to the polymer solution or precipitant for, that is, influencing pore formation.[28] Choosing the preparation conditions as well as the polymer solution composition properly allows engineering complex porosity, integrating combinations of porosity gradients, skin layers and macrovoids. Almost exclusively, this preparation method has been applied to thin porous layers as used in membrane filtration and battery separators or to hollow fiber production. Monolithic geometries are very challenging to produce as macrovoids occur when the porosity surpasses a certain thickness.[31]

In this work, we first identify a polymer/solvent system that allows us to prepare homogeneous porosity throughout the whole monolith without inducing macrovoid formation. A PVDF concentration ranging from 15 to 25 wt% is used for the casting solution, and aprotic solvents such as triethyl phosphate (TEP) and N-methyl-2-pyrrolidone (NMP) were chosen to prepare the PVDF solution. Water and ethanol were used as precipitants, as both are miscible with the solvents TEP and NMP and serve as non-solvents for the polymer. First casting processes were carried out in transparent cuvettes to investigate
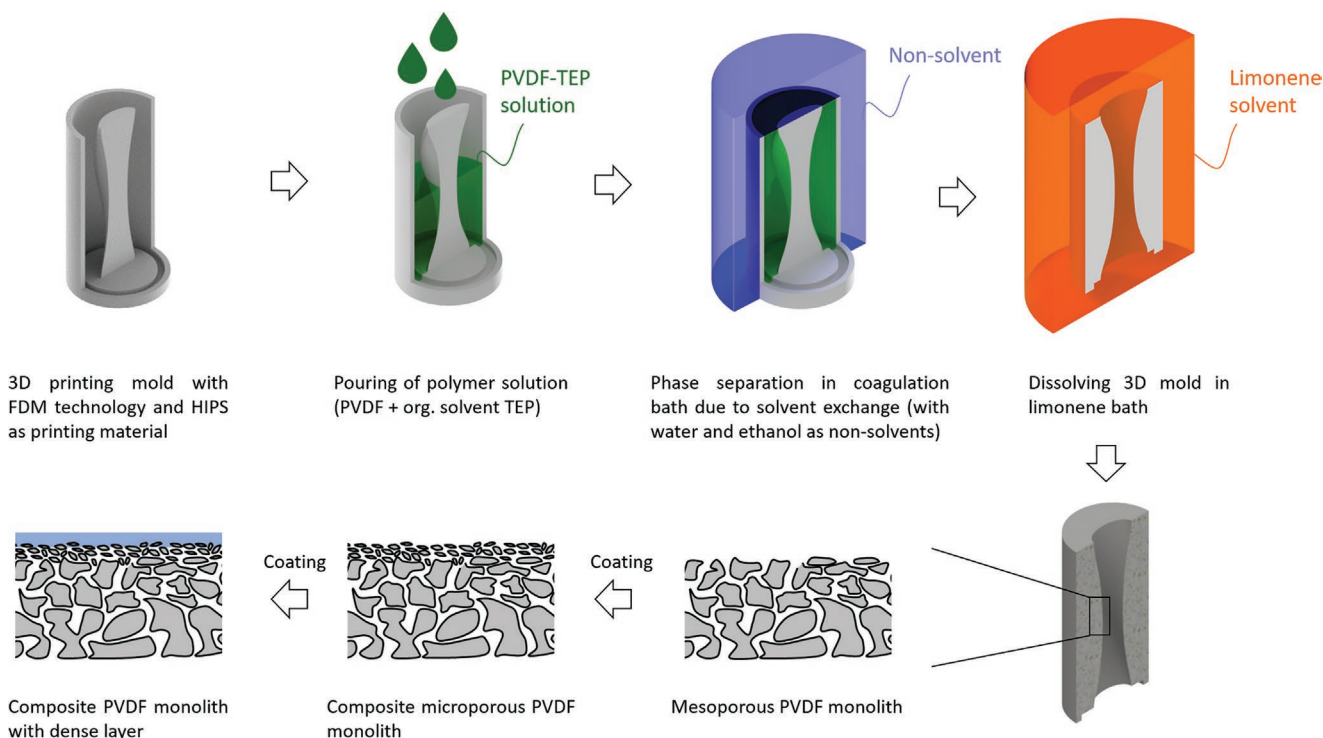
Figure 1. Visualization of the presented step-wise casting process for fabricating 3D membranes including the steps 3D printing molds, pouring of polymer solution in a 3D mold, non-solvent induced phase separation process, and afterwards dissolution of the mold. The porous PVDF bodies are then further coated to tune porosity and obtain a gas-selective layer. A helix body was chosen as an example. The manufacturing process can be applied to a wide range of architectures.

the NIPS process in a simple and easily accessible mold as done for the first chromatography monoliths.[22]

The polymer concentration was varied and analyzed concerning membrane morphology (**Figure 2**). In the resulting monolith, a uniform pore distribution was observed, independent of the three polymer concentrations tested (Figure 2a). A solid body with uniform pores was successfully achieved with the phase inversion process. Overall, no correlation between morphology and polymer content in the casting solution can be identified. The influence of polymer concentration on membrane morphology seems not to apply under these preparation conditions, which differs from literature.[28,32]

Three sections of the cuvette monoliths were analyzed to study the morphologies stemming from the phase inversion process. Figure 2b shows exemplary SEM images of the top, bottom and sidewall, respectively. The precipitation in longitudinal direction seems uniform and even the membrane morphology is similar in the top and bottom positions. Due to the decreased solvent exchange rate with increasing diffusion path, precipitation significantly slows down towards the bottom part. Hence, it was expected that the monolith shows a different morphology. However, the top and bottom show the same typical amorphous structure regardless of the lateral position. The phase inversion process takes 40 h to complete due to the diffusion limitation of the solid block. A kinetics analysis can be found in Supporting Information S1, as well as an analysis of the influence of additives on the pore formation in Supporting Information S2.

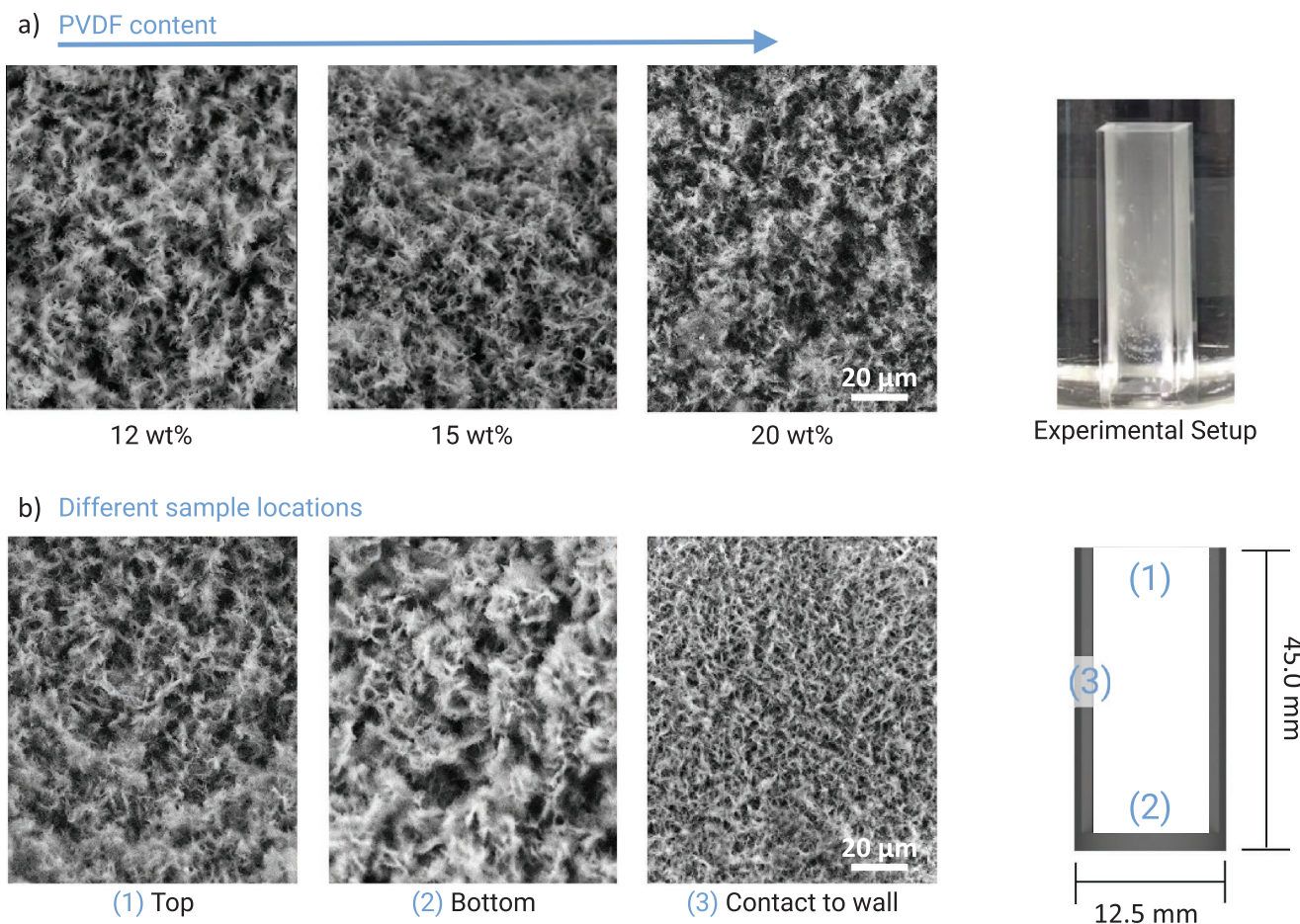In contrast to homogeneous precipitation in the longitudinal direction, the membrane morphology at the outer surface shows smaller pores, formed by a faster solvent exchange rate. This morphology difference could be explained by the shrinking of the membrane during phase inversion leading to a small gap between the wall and the precipitated membrane. This gap allows an inflow of the non-solvent, which leads to a decreased diffusion path resulting in a faster solvent and non-solvent exchange.

This process demonstrates that a molding process with a suitable NIPS recipe is capable of producing 3D PVDF monoliths of uniform porosity.

2.2. PVDF Coating of Porous PVDF Monoliths

The coating of the PVDF monoliths enables the change of surface porosity towards smaller pores and enables an asymmetric membrane architecture. Not only for size-exclusion applications but also for achieving smooth PDMS coatings for contactor applications, finer surface porosity is desired. A 15 wt% PVDF solution was used for the PVDF coating, like in the monolith fabrication. However, the solvent TEP used for monolith fabrication did not provide a stable PVDF layer (see Figure S4, Supporting Information). The PVDF coating was not stable and peeled off. In contrast to that, the use of NMP led to a homogeneous and stable layer with good adhesion to the surface. For this reason, the polymer solution was prepared with the solvent NMP.

Figure 3 illustrates the coagulation environment's impact on coating morphology for a fixed polymer concentration (15 wt% PVDF). Ethanol and water were used as precipitants and led to entirely different results (Figure 3a). Phase inversion in water

2100325 (3 of 9)

**ADVANCED
SCIENCE NEWS**

www.advancedsciencenews.com

**ADVANCED
MATERIALS
TECHNOLOGIES**

www.advmattechnol.de

Figure 2. a) SEM images of porous monoliths with increasing PVDF polymer content. The images were taken from the central top position (1). PVDF was dissolved in TEP in three different concentrations 12, 15, 20 wt% and molded in cuvette bodies. Precipitation was performed first in ethanol (20 °C, 18 h) and afterwards substituted with H_2O (40 °C). b) SEM images from different positions of the cuvette-shaped monoliths: top, bottom and contact to the wall of the mold.

led to a well-defined and stable layer, composed of a porous middle part followed by a macrovoid layer and a dense top layer. Contrary to that, ethanol led to a sponge-like layer, which can be explained by the slower solvent exchange rate (see mean phase inversion velocities of ethanol and water in Figure S2, Supporting Information). The coagulation with water resulted in a well-defined coating layer and thus was selected as a suitable precipitant for the PVDF coating. Another important parameter of the NIPS process is the coagulation bath temperature. Increasing temperature is known to influence the phase inversion process due to faster solvent exchange rates and thus faster precipitation. Therefore, phase inversion was tested for the coagulation bath medium water at 20 °C and 40 °C. For both conditions, a uniform layer was achieved.
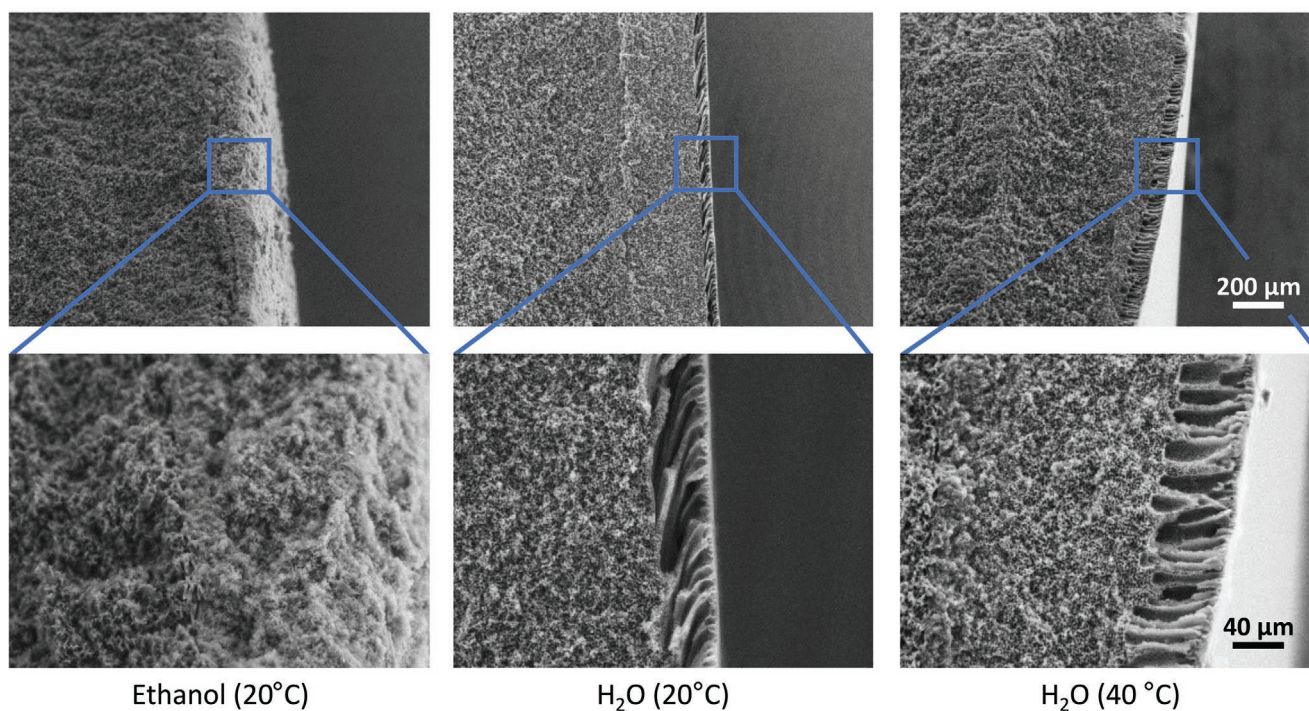
Beyond that, the addition of additives in the coagulation medium water was further investigated and visualized in Figure 3b. Solvent fractions of NMP in the non-solvent water suppressed the formation of macrovoids, and a sponge-like structure remained. Jung et al. obtained similar results where an increasing fraction of solvent in the coagulation bath led to a suppression of macrovoid formation.[32] The decreased concentration gradient between polymer solution (85 wt% NMP)

and coagulation bath (60 wt% NMP as an additive in water) results in a reduced mass exchange rate. This phenomenon is known in literature.[28,30] Agar and agarose were used as additives and affected even in small fractions (0.1 wt%) the coagulation bath's viscosity. With the addition of agar and agarose, diffusion was purposefully reduced (Figure 3b), but macrovoids still developed during precipitation. Like pure water, the macrovoids were elongated, which can be explained by the reduced precipitation kinetics. Temperature and viscosity can, therefore, significantly influence the precipitation reaction. To summarize, the precipitation bath deserves special attention in the post-treatment of 3D PVDF structures. It showed that additives in the coagulation bath have a significant influence on the yielded PVDF layer.

2.3. PDMS Coating of Composite Monoliths

In order to obtain a 3D gas diffusion membrane suitable for contactor applications, the PVDF coated PVDF monoliths were coated with a layer of PDMS. PDMS is a dense, silicon-based polymer with excellent gas transfer properties for respiratory gases.[33] A direct coating of the macroporous PVDF structures

**ADVANCED
SCIENCE NEWS**

www.advancedsciencenews.com

**ADVANCED
MATERIALS
TECHNOLOGIES**

www.advmattechnol.de

a) Impact of temperature and coagulation bath medium (water and ethanol) on coated layer

b) Impact of additives in coagulation bath (water) on coated layer
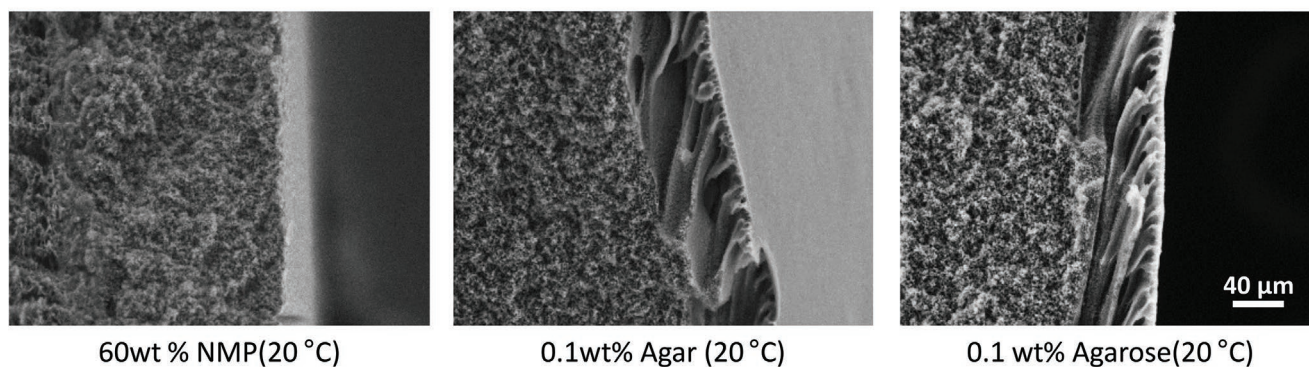
Figure 3. a) SEM images of coated PVDF layer on PVDF monoliths with varying parameters of precipitation agent and temperature, and b) fraction of additives in the coagulation bath.
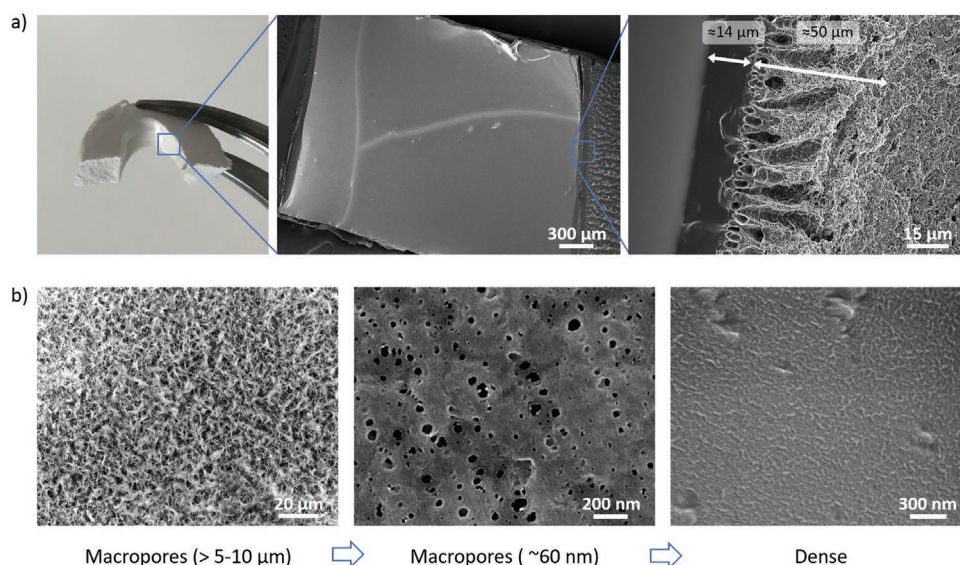
did not lead to a successful coating with PDMS (see Figure S5, Supporting Information). Jie et al. successfully coated PVDF hollow fibers with PDMS, but the initial size of the PVDF pores (0.16 μm) was significantly smaller than in the investigated samples here (5–10 μm).[34] Smaller pores are required to gain a surface more suitable for PDMS coating. For this reason, the PVDF monoliths were pre-coated with PVDF to obtain smaller pores.

PDMS was then successfully applied on a porous 3D PVDF monolith pre-coated with PVDF (**Figure 4**a). A stable and homogeneous PDMS layer with a thickness of around 14 μm was obtained by centrifuging the PDMS solution into the PVDF coated PVDF monolith. With the presented coating techniques, one can now tune the pore size from 5–10 μm to around 60 nm to even dense skin layers (Figure 4b).

2.4. Fabricating Complex Geometries

Besides the successful production of simple 3D membranes, experiments were conducted to check the feasibility of the manufacturing process for more complex structures and designs. For this purpose, 3D molds were engineered and produced with additive manufacturing.

Figure 5 shows successfully manufactured porous geometries of different levels of complexity. A detailed observation of the membrane morphology (Figure 5a) displays an overall symmetric bicontinuous structure throughout the whole membrane body. Since phase inversion is slow, the overall structure of the 3D bodies is sponge-like. On closer examination of the PVDF structure, small filaments reveal at the end of a branch

**ADVANCED
SCIENCE NEWS**

www.advancedsciencenews.com

**ADVANCED
MATERIALS
TECHNOLOGIES**

www.advmattechnol.de

Figure 4. a) PDMS coating of a PVDF helix monolith with previous PVDF coating. Photograph (left image), SEM images (middle, right). b) SEM images of the three subsequent fabrication steps, namely monolith fabrication, PVDF coating and PDMS gas-diffusion layer. The base PVDF helix monolith was prepared with 15 wt% PVDF and 85 wt% TEP, coagulation bath ethanol (20 °C, 18 h) and afterwards water (40 °C). The subsequent coating with PVDF was carried out with 15 wt% PVDF and 85 wt% NMP, and water (20 °C, 18 h) as coagulation bath. The final coating with PDMS was performed in PDMS mixed with cross-linker (7:1) and afterwards diluted in hexane (1:1). After centrifuging, the PDMS was cured (60 °C, overnight).
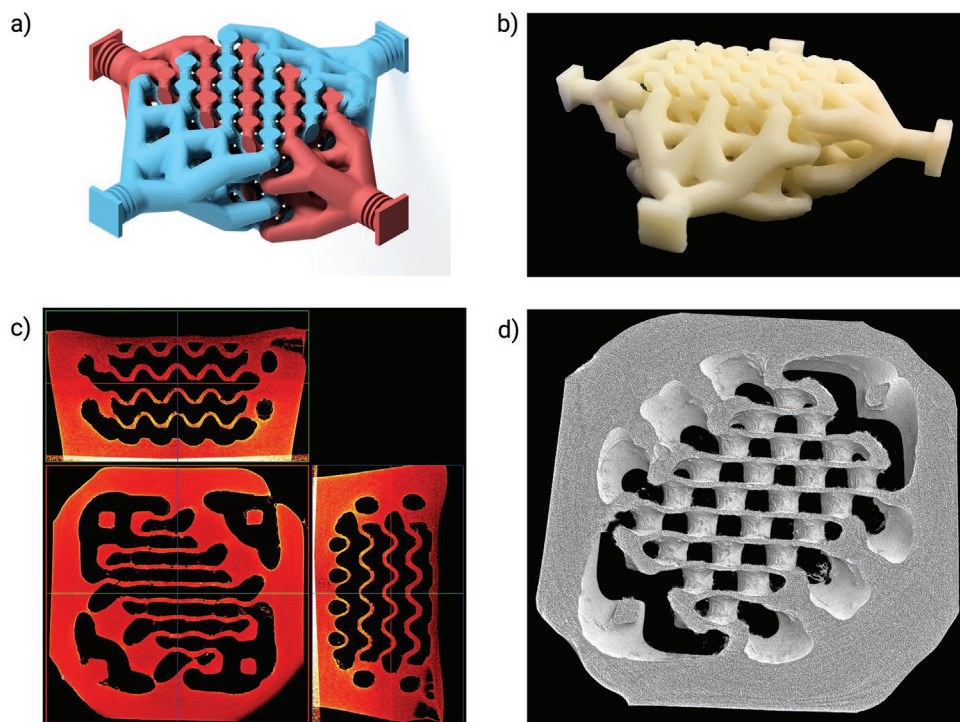
(Figure 5a). Presumably, these filaments developed because of the semi-crystalline morphology of PVDF. However, since the diffusion paths for solvent exchange are quite long, compared to conventional NIPS processes in hollow fiber and flat sheet membrane manufacturing, the solvent exchange is substantially delayed and overlaps with crystallization phenomena. Thus, regions of crystalline and amorphous structure coexist.[28,35,36] From a simple helix body to more complex structures, Figure 5b shows that the fabrication process developed is adaptable to a wide range of printable geometries, such as TPMS (Gyroid, Schwarz-P and Schwarz-D).

To demonstrate the strength and applicability of this process, we fabricated the first 3D templated TPMS membrane module monolith. **Figure 6**a shows the design of the casting core with
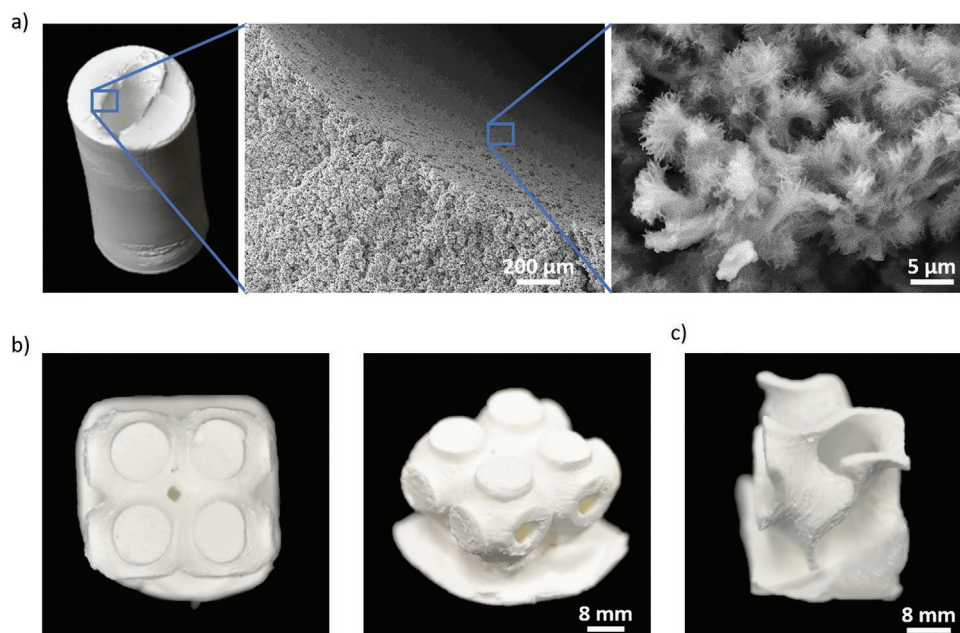
Figure 5. Fabrication of complex porous PVDF based monoliths. a) Helix body with an amorphous and crystalline structure, TPMS based b) schwarz-P and c) gyroid structure. The gyroid structure has an edge length of 26 mm, and the 2 × 2 schwarz-P structure of 37 mm, respectively. SEM images were taken from a cross-sectional view. Bodies were fabricated using a polymer solution consisting of PVDF 15 wt% and TEP 85 wt%. Precipitation was performed first in ethanol (20 °C, 18 h) and afterward in H_2O (40 °C).

**ADVANCED
SCIENCE NEWS**

www.advancedsciencenews.com

**ADVANCED
MATERIALS**
TECHNOLOGIES

www.advmattechnol.de

Figure 6. Design, fabrication, and analysis of a porous PVDF Monolith with $2 \times 2 \times 2$ Schwarz-D TPMS internal channel-structure. The monolith was prepared with 15 wt% PVDF and 85 wt% TEP, coagulation bath ethanol (20 °C, 18 h) and afterwards water (40 °C). Maximum length is 40 mm. Void volume of the channels is ≈1.8 mL with an internal surface area of 3.5 cm². Black area represents void space. a) Rendering of the internal fluidic structure with the two-fluid compartments colored in red and blue with the void being filled with polymer solution forming the body and the membrane separating the two flow channels. b) photography of the printed casting core c) μ-CT analysis of the resulting PVDF monolith in *x*, *y*, and *z* sectional view. The color scale shows local material density from red (low density) to yellow (high density). d) μ-CT image view through a slice of the monolith.

the fluid compartments in red and blue. The core was designed with 2x2x2 Schwarz-D geometry leading to intricately intertwined fluid compartments that were equipped with flow distributing inlet and outlet connections. The resulting 3D-printed casting core, shown in Figure 6b, is integrated into the mold to fabricate the PVDF membrane module monolith.

A non-invasive μ-CT analysis of the TPMS membrane module, presented in Figure 6c and d, demonstrates a perfect representation of the Schwarz-D structure. While the cut views in Figure 6c show slight qualitative differences in material density (yellow areas), the material distribution and porosity seem to be homogeneous and is defect-free. In Figure 6d, a digitally cut slice of the module shows that the TPMS template left a spectacular surface quality, ideally suited for subsequent coating procedures.

3. Conclusion

This work describes an entirely novel approach to produce 3D TPMS membrane modules. The manufacturing process is adaptable to a wide range of printable molds and a continuous porous structure realized with NIPS technology. With this development, the NIPS process has overcome its limitation for hollow-fiber and flat-sheet membrane manufacturing. Furthermore, advanced coating techniques offer more degrees of freedom regarding membrane porosity and process application. We further identified essential parameters typical for

NIPS processes and studied their impact on the monolith's membrane morphology.

With emerging development in additive manufacturing, mold processing will benefit from improving the resolution and precision of 3D printers and thus supporting increasingly flexible membrane manufacturing techniques. Furthermore, additive manufacturing will be an essential pillar in module construction since the novel membrane geometries require a novel module and housing design.

Further work has to be done to characterize the newly developed 3D membranes' performance concerning membrane resistance (pure water flux), mass transport properties, and susceptibility to fouling. Apart from the membrane performance, it will be of high relevance to test the suitability of the novel designed membranes for membrane oxygenators. With this freedom of design, the membrane architecture for blood oxygenators can be wholly rethought and optimized against dead zones with improved fluid designs for the shear-sensitive blood. However, the scalability towards a larger membrane area (e.g., membrane oxygenators currently require 1.8 m² blood-contacting area) will be challenging regarding manufacturing time.

4. Experimental Section

Preparation of Polymer Solution: PVDF pellets ($M_w = 530$ kDa, Sigma-Aldrich, USA) were dissolved in triethyl phosphate (TEP) (≥99%, Merck KGaA, Germany) or in *N*-Methyl-2-pyrrolidone (NMP) (≥99.5%,

**ADVANCED
SCIENCE NEWS**

www.advancedsciencenews.com

**ADVANCED
MATERIALS
TECHNOLOGIES**

www.advmattechnol.de

Thermo Fisher Acros Organics, Belgium). The additives dehumidified lithium chloride (LiCl) (≥99%, Sigma-Aldrich, USA) and Pluronic F127 (Sigma-Aldrich, USA) were used. The polymer solution was protected against the environment by a septum and heated up. The temperature was adjusted to 60 °C and controlled by a thermostat (Hei-Con EKT 3001, Heidolph Instruments GmbH & Co. KG, Germany). A magnetic stirrer constantly mixed the solution until the PVDF pellets dissolved. The polymer solution was placed in a water bath for uniform heating. Afterward, the solution was stored at 20 °C until usage.

3D Printing Mold: The manufacturing process of 3D membranes started with the computer-aided design of membrane geometries. The complex TPMS structures were designed as described in ref. [15]. First, the surface-generator tool K3dSurf was used to generate surfaces based on the mathematical equations for schwarz-P and gyroid. Two surfaces were generated and shifted by a defined distance. A volume between both surfaces was built, which represented the bulk thickness. The object was saved as .obj-file and further processed in Blender (version 2.82, www.blender.org) to create interconnected front surfaces. The outlines were connected, and the structures were scaled to the desired dimensions. The object was then exported as a .stl-file and further processed in Autodesk Inventor (version Inventor 2019, Autodesk, US). With the add-in Mesh Enabler, the surface was converted into a base feature editable in Autodesk Inventor. A second, larger body was added to the CAD file, and the TPMS structure was subtracted therefrom so that the negative mold was formed. The negative molds were 3D printed using FDM technology (Ultimaker 3, NL). The structures were printed in an upright position along their longitudinal axis to minimize overhangs, using LimoSolve, high impact polystyrene (HIPS) (Formfutura BV, NL). Besides the 3D printed molds and casting cores, transparent polystyrene-based cuvettes were used as easily accessible molds to study the non-solvent induced phase separation process.

Casting Process for Porous Polymeric PVDF Monoliths: The step-wise casting process for the fabrication of 3D monoliths is depicted in Figure 1. Before casting, the polymer solution was centrifuged (5804 R, Eppendorf AG, Germany) at 2600 to 3200 rpm to eliminate air bubbles. Afterward, the polymer solution was slowly cast into the mold. The filled molds were immersed in a coagulation bath to promote phase inversion due to solvent exchange. The coagulation bath consisted of only ethanol. After 1 day, ethanol was replaced with distilled water. The coagulation bath was replaced regularly and continuously mixed with a magnetic stirrer. After complete phase separation, the mold material HIPS was dissolved in the solvent limonene (≥93.0%, Sigma-Aldrich, USA). The solution was stirred and heated up to 40 °C to accelerate the dissolving process. Afterward, the monolith was immersed in distilled water for one day to remove limonene residuals inside the macroscopic pores. The monolith was cooled down overnight to −21 °C and afterward further cooled down with liquid nitrogen. Finally, the monolith was freeze-dried overnight to sublimate the remaining water and prevent the pores inside the PVDF material from collapsing.

Coating of Porous PVDF Monoliths: The monolithic base structure was coated with PVDF and PDMS to achieve more narrow pores or even a gas selective layer. Before coating, the polymer solution was centrifuged at 2600–3200 rpm to remove air bubbles (5804 R, Eppendorf AG, Germany). The cuvette-shaped monoliths were dip-coated in the desired coating solution with a custom-made dip-coating station. The sample was fixed using a gripper, which was connected to a motor. The moving speed into and out of the coating solution was set to 10 mm s^{-1}. The sample was then immersed in the coating solution (varying PVDF contents 5–15 wt% in either TEP or NMP solvent) for 30 s. After 30 s, the coated monolith was pulled out and transferred in a stirred and temperature-controlled (40 °C) coagulation bath for non-induced phase separation. Different solvents (ethanol, water) and additives in the solvents (0.1 wt% agar or agarose) were tested as a coagulation bath medium. PDMS coating was performed in a diluted PDMS/hexane solution (1:1) (Sylgard 184 silicon elastomer and curing agent, Dow Corning, USA) and dip-coated (10 mm s^{-1}, 30 s). The PDMS was afterward cured at 60 °C. Contrary to the cuvette-shaped monoliths, the coating process for the 3D printed structures was carried out in a centrifugation

process (5804 R, Eppendorf AG, Germany). The 3D samples were placed in a falcon tube containing a spacer at the bottom, which allowed a drain of surplus coating solution during centrifugation. The coating solution was applied in a custom-made funnel and placed on top of the 3D body to only coat the lumen side of the sample. Centrifugation was performed at 30 s and 1000 rpm. The further processing in a coagulation bath for PVDF coating or the successive curing for PDMS coating was performed in the same way as described for the dipping process.

Analytics: Scanning electron microscopy (SEM) was used for visual evaluation of the produced monoliths. The sample was submerged in liquid nitrogen to cool down and to become brittle. The sample was then broken by using two tweezers. SEM images were taken from the fractured edges at 5 kV and 5 μA on a Hitachi SU4800. Before imaging, the monoliths were sputtered with 7 nm of a gold-palladium alloy (60 : 40) (Sputtercoater EM ACE600, Leica).

The 3D monoliths were scanned with computed tomography (SKYSCAN1272, Bruker Corporation) to analyze the fabricated 3D structures non-invasively.

Supporting Information

Supporting Information is available from the Wiley Online Library or from the author.

Conflict of Interest

The authors declare no conflict of interest.

Data Availability Statement

The data that support the findings of this study are available from the corresponding author upon reasonable request.

[1] C. Fritzmann, M. Hausmann, M. Wiese, M. Wessling, T. Melin, *J. of Membrane Sci.* **2013**, *446*, 189.

[2] C. Fritzmann, M. Wiese, T. Melin, M. Wessling, *J. of Membrane Sci.* **2014**, *463*, 41.

[3] S. Armbruster, O. Cheong, J. Lölsberg, S. Popovic, S. Yüce, M. Wessling, *J. of Membrane Sci.* **2018**, *554*, 156.

[4] J. Lölsberg, O. Starck, S. Stiefel, J. Hereijgers, T. Breugelmans, M. Wessling, *ChemElectroChem* **2017**, *4*, 3309.

[5] S. Armbruster, A. Brochard, J. Lölsberg, S. Yüce, M. Wessling, *J. of Membrane Sci.* **2019**, *570-571*, 537.

[6] T. Femmer, M. L. Eggersdorfer, A. J. C. Kuehne, M. Wessling, *Lab on a Chip* **2015**, *15*, 3132.

[7] M. Wiese, S. Benders, B. Blümich, M. Wessling, *Chem. Eng. J.* **2018**, *343*, 54.

[8] T. Luelf, D. Rall, D. Wypysek, M. Wiese, T. Femmer, C. Bremer, J. U. Michaelis, M. Wessling, *J. of Membrane Sci.* **2018**, *555*, 7.

[9] T. Luelf, M. Tepper, H. Breisig, M. Wessling, *J. of Membrane Sci.* **2017**, *533*, 302.

[10] M. Wiese, O. Nir, D. Wypysek, L. Pokern, M. Wessling, *J. of Membrane Sci.* **2019**, *569*, 7.

[11] T. Femmer, A. J. C. Kuehne, M. Wessling, *Lab on a Chip* **2014**, *14*, 2610.

[12] J.-Y. Lee, W. S. Tan, J. An, C. K. Chua, C. Y. Tang, A. G. Fane, T. H. Chong, *J. of Membrane Sci.* **2016**, *499*, 480.

[13] Z.-X. Low, Y. T. Chua, B. M. Ray, D. Mattia, I. S. Metcalfe, D. A. Patterson, *J. of Membrane Sci.* **2017**, *523*, 596.

[14] S. C. Kapfer, S. T. Hyde, K. Mecke, C. H. Arns, G. E. Schröder-Turk, *Biomaterials* **2011**, *32*, 6875.

[15] T. Femmer, A. J. C. Kuehne, M. Wessling, *Chem. Eng. J.* **2015**, *273*, 438.

[16] T. Femmer, A. J. C. Kuehne, J. Torres-Rendon, A. Walther, M. Wessling, *J. of Membrane Sci.* **2015**, *478*, 12.

[17] J. Arens, O. Grottke, A. Haverich, L. S. Maier, T. Schmitz-Rode, U. Steinseifer, H. P. Wendel, R. Rossaint, *ASAIO J.: Artif. Org. Res. and Develop.* **2020**, *66*, 847.

[18] H. J. Eash, H. M. Jones, B. G. Hattler, W. J. Federspiel, *ASAIO J.* **2004**, *50*, 491.

[19] W. J. Federspiel, K. A. Henchir, *Encyclopedia of Biomaterials and Biomedical Engineering*, Marcel Dekker; New York **2004**, pp. 910–921.

[20] C. Fee, S. Nawada, S. Dimartino, *J. of Chromatography A* **2014**, *1333*, 18.

[21] J. Lölsberg, A. Cinar, D. Felder, G. Linz, S. Djeljadini, M. Wessling, *Small* **2019**, *15*, 1970177.

[22] F. Svec, *J. of Sep. Sci.* **2009**, *32*, 3.

[23] S. Xie, R. W. Allington, J. M. J. Fréchet, F. Svec, *Porous Polymer Monoliths: An Alternative to Classical Beads*, Springer Berlin Heidelberg, **2002**, pp. 87–125.

[24] I. Nischang, T. J. Causon, *TrAC Trends in Anal. Chem.* **2016**, *75*, 108.

[25] J. Linkhorst, K. Percin, S. Kriescher, M. Wessling, *ChemElectroChem* **2017**, *4*, 2760.

[26] Z. Dong, H. Cui, H. Zhang, F. Wang, X. Zhan, F. Mayer, B. Nestler, M. Wegener, P. A. Levkin, *Nat. Commun.* **2021**, *12*, 1.

[27] M. Mulder, *Basic Principles of Membrane Technology*, 2nd ed., Springer, Dordrecht, the Netherlands **1996**.

[28] G. R. Guillen, Y. Pan, M. Li, E. M. V. Hoek, *Ind. & Eng. Chem. Res.* **2011**, *50*, 3798.

[29] Z. Cui, E. Drioli, Y. M. Lee, *Prog. in Polym. Sci.* **2014**, *39*, 164.

[30] H. Strathmann, K. Kock, *Desalination* **1977**, *21*, 241.

[31] M. Bikel, I. G. Pünt, R. G. Lammertink, M. Wessling, *ACS Appl. Mater. and Interfaces* **2009**, *1*, 2856.

[32] J. T. Jung, J. F. Kim, H. H. Wang, E. di Nicolo, E. Drioli, Y. M. Lee, *J. of Membrane Sci.* **2016**, *514*, 250.

[33] T. C. Merkel, V. I. Bondar, K. Nagai, B. D. Freeman, I. Pinnau, *J. of Polym. Sci. Part B: Polym. Phys.* **2000**, *38*, 415.

[34] Y. Jie, Z. Dandan, Y. Shuren, Y. Hong, D. Ziwei, L. Biaoming, Y. Zhou, W. Zhongwei, S. V. Agtmaal, F. Chunhui, H. Bangjun, *J. of Membrane and Sep. Technol.* **2013**, *2*, 163.

[35] N. Peng, N. Widjojo, P. Sukitpaneenit, M. M. Teoh, G. G. Lipscomb, T.-S. Chung, J.-Y. Lai, *Prog. in Polym. Sci.* **2012**, *37*, 1401.

[36] T.-H. Young, L.-P. Cheng, D.-J. Lin, L. Fane, W.-Y. Chuang, *Polymer* **1999**, *40*, 5315.